Proceedings of the Combustion Institute SAND2020-1364C

Identification of combustion mode under MILD conditions using Chemical Explosive Mode Analysis

--Manuscript Draft--

Manuscript Number:	PROCI-D-19-01775
Article Type:	14. CC/CCC Submissions
Keywords:	MILD combustion; turbulent combustion; CEMA; Ignition; deflagration
Corresponding Author:	Nguyen Anh Khoa Doan, Ph.D. Technical University of Munich Garching, GERMANY
First Author:	Nguyen Anh Khoa Doan, Ph.D.
Order of Authors:	Nguyen Anh Khoa Doan, Ph.D.
	Shubhangi Bansude
	Kosuke Osawa, Dr.
	Yuki Minamoto, Ph.D.
	Tianfeng Lu, Prof.
	Jacqueline H. Chen, Dr.
	Nedunchezhian Swaminathan, Prof.
Abstract:	p, li { white-space: pre-wrap; } Direct Numerical Simulations (DNS) data of Moderate or Intense Low-oxygen Dilution (MILD) combustion are analysed to identify the contributions of the autoignition and flame modes. This is performed using an extended Chemical Explosive Mode Analysis (CEMA) which accounts for diffusion effects allowing it to discriminate between deflagration and autoignition. This analysis indicates that in premixed MILD combustion condition, the main combustion mode is ignition for all dilution and turbulence levels and for the two reactant temperature conditions considered. In non-premixed condition, the preponderance of the ignition mode was observed to depend on the axial locations and mixture fraction stratification. With a large mixture fraction lengthscale, ignition is more preponderant in the early part of the domain while the deflagrative mode increases further downstream. On the other hand, when the mixture fraction lengthscale is small, sequential autoignition is observed. Finally, the various combustion modes are observed to correlate strongly with mixture fraction where lean mixtures are more likely to autoignite while stoichiometric or rich mixtures are more likely to react as deflagrative structures.

Identification of combustion mode under MILD conditions using Chemical Explosive Mode Analysis

N. A. K. Doan[a,e,*], S. Bansude[b], K. Osawa[c], Y. Minamoto[c], T. Lu[b], J. H. Chen[d], N. Swaminathan[e]

[a] *Department of Mechanical Engineering and Institute for Advanced Study, Technical University of Munich, Garching, Germany*
[b] *Department of Mechanical Engineering, University of Connecticut, Storrs, USA*
[c] *Department of Mechanical Engineering, Tokyo Institute of Technology, Meguro-ku, Japan*
[d] *Combustion Research Facility, Sandia National Laboratory, Livermore, USA*
[e] *Department of Engineering, University of Cambridge, Cambridge, UK*

Abstract

Direct Numerical Simulations (DNS) data of Moderate or Intense Low-oxygen Dilution (MILD) combustion are analysed to identify the contributions of the autoignition and flame modes. This is performed using an extended Chemical Explosive Mode Analysis (CEMA) which accounts for diffusion effects allowing it to discriminate between deflagration and autoignition. This analysis indicates that in premixed MILD combustion condition, the main combustion mode is ignition for all dilution and turbulence levels and for the two reactant temperature conditions considered. In non-premixed condition, the preponderance of the ignition mode was observed to depend on the axial locations and mixture fraction stratification. With a large mixture fraction lengthscale, ignition is more preponderant in the early part of the domain while the deflagrative mode increases further downstream. On the other

*Corresponding author:
Email address: doan@tfd.mw.tum.de (N. A. K. Doan)

hand, when the mixture fraction lengthscale is small, sequential autoignition is observed. Finally, the various combustion modes are observed to correlate strongly with mixture fraction where lean mixtures are more likely to autoignite while stoichiometric or rich mixtures are more likely to react as deflagrative structures.

Keywords: MILD Combustion, Turbulent Combustion, CEMA, ignition, deflagration

---

1. Introduction

There is a growing interest in Moderate or Intense Low-oxygen Dilution (MILD) combustion, also called flameless combustion, to mitigate pollutants production and increase thermal efficiency [1, 2]. This is because of the well distributed reactions found in MILD combustion which yield low temperature gradients, low NO_x production, high stability and low acoustic oscillations in MILD combustion burners [1–3]. The particular conditions for MILD combustion are typically achieved by diluting the reactants with exhaust gases. By using exhaust gas recirculation (EGR), the reactants temperature is increased to a temperature T_r larger than the mixture autoignition temperature T_{ign} while the temperature increase during combustion, ΔT, remains smaller than T_{ign} because of the dilution of the reactant mixtures. Indeed, reactant mixtures in MILD combustion have low oxygen content, typically 5% or less by volume [1].

Due to these particular conditions, the physical understanding of MILD combustion is challenging. In particular, both features of propagating flames

and ignition have been observed in MILD combustion. Indeed, OH- Planar Laser-Induced Fluorescence (PLIF) images have shown the presence of flame-like structures, with thin regions with clear OH gradients [4, 5]. In addition, in a Jet in Hot Coflow (JHC) configuration, CH_2O-PLIF also showed the production of ignition kernels due to the heated coflow, a process which was key in sustaining reactions [5, 6]. This was also further emphasized using UV-luminescence images in a JHC configuration [7] or OH^* images of a Jet in Hot Crossflow configuration [8]. Thus, this balance between ignition and propagating flames in MILD combustion requires further investigations to improve the understanding of MILD combustion and also to understand its impact on the modelling framework for MILD combustion.

Recent Direct Numerical Simulations (DNS) of MILD combustion have been conducted in previous studies [9–12]. In the igniting mixing layer between methane and diluted hot air configuration of [12], the existence of autoignition along the iso-surface of the most reactive mixture fraction, Z_{MR}, was highlighted. Furthermore, it was observed that most reactions occurred through ignition at various spatial locations at Z_{MR}, and at different times depending on the local temperature and scalar dissipation rate, and not through the development of these kernels into propagating flames. Other DNS of premixed MILD combustion with internal EGR showed frequent interactions of reaction zones and highlighted the co-existence of ignition kernels and propagating flames where the former were present to a greater extent in the upstream regions [9]. The work of [11] further showed that, in non-premixed MILD combustion with internal EGR, the most probable combustion modes are also dependent on the mixture fraction variation:

the existence of sequential autoignition is favoured when the characteristic lengthscale of the mixture fraction field, ℓ_Z is similar to the chemical lengthscale ℓ_c, while the development of propagating flames is more probable if $\ell_c > \ell_Z$. This further emphasises the importance of understanding the balance between ignition and propagating flames and how the transition occurs between the various combustion modes.

To this aim, a recent approach, based on Chemical Explosive Mode Analysis (CEMA) has been proposed to distinguish ignition and deflagration [13] and used to analyse DNS data of a sequential combustor configuration [14] and high Karlovitz number flames [15]. CEMA is based on eigen-analysis and has already been used to identify premixed flame fronts, mixing, ignition, local extinction and to distinguish between premixed and non-premixed combustion [16–18]. Furthermore, it was shown to be a robust indicator for ignition [19]. Therefore, this suggests that CEMA is suitable to analyse the combustion modes under MILD conditions.

Thus, the present work analyses the premixed and non-premixed MILD combustion DNS of [9] and [10] using the CEMA method presented in [13] to identify and quantify the importance of each combustion mode. The paper is organised as follows. The DNS data and its methodology are summarized in the next section. Then, the analysis method based on CEMA is presented. The results of CEMA on laminar flames and on MILD combustion DNS are presented and discussed in section 4. The main findings are summarised in the final section.

2. DNS Methodology

The DNS data generated in [10] and [9] for non-premixed and premixed MILD combustion with internal EGR, respectively, are used for this work. These are DNS of MILD combustion at atmospheric pressure of methane and air diluted with exhaust gases inside a cubic domain. For both conditions, the procedure to generate the initial fields is split into two phases detailed in [9, 10]. First, initial fields are generated to mimick a distribution of burnt and unburnt gases, and with mixture fraction distribution for the non-premixed cases. Then, a mixing DNS is simulated without chemical reactions in a periodic domain for about one large eddy turnover time (shorter than the minimum ignition delay time) to ensure that the scalar and flow fields have interacted sufficiently before the combustion commences. This reproduces the conditions obtained from EGR found in MILD combustion. In the second stage, this inhomogeneous mixture is used as the initial and inflowing mixture for the combustion simulation. Further details are presented in [9, 10].

Three non-premixed and four premixed cases, described in Tables 1, 2 and 3, are considered here. All cases, except case C1, have already been presented in previous studies [9, 10] and their characteristics are summarised here. Case C1 is described further below. All these cases have similar turbulence field apart from cases A2 and C1 which are less turbulent as described in Tables 3. Three different levels of dilution are considered here as described in Table 2 enabling the effect of O_2 dilution on the combustion mode to be assessed. Finally, the cases AZ1 and AZ2 differed by the length scale ratio, ℓ_Z/ℓ_c, of mixture fraction, Z, and progress variable, c, to study the influence of mixture fraction stratification on MILD combustion. The effect of reactant

temperatures is also studied with the additional case C1 which has a lower reactant temperature with $T_r = 1300$ K and which is a premixed MILD combustion case. All cases have an average equivalence ratio of $\phi = 0.8$.

Table 1: DNS initial conditions. P and NP respectively stand for premixed and non-premixed conditions. X_{O_2} denotes the mole fraction of O_2, $\langle\cdot\rangle$ the volume average, σ the standard deviation of the specified quantity.

Case	P/NP	Mech	Λ_0/ℓ_Z	$\langle X_{O_2}\rangle$	$X_{O_2}^{max}$	ℓ_Z/ℓ_c	$\langle Z\rangle$	Z_{st}	σ_Z	$\langle c\rangle$	σ_c
AZ1	NP	MS-58	0.60	0.0270	0.035	1.30	0.008	0.010	0.0084	0.56	0.26
AZ2	NP	MS-58	0.79	0.0285	0.035	1.01	0.008	0.010	0.0105	0.56	0.28
BZ1	NP	MS-58	0.60	0.0160	0.020	1.30	0.0046	0.0058	0.0057	0.56	0.26
A1	P	Smooke	-	0.0350	0.048	-	0.011	0.014	-	0.50	0.3
A2	P	Smooke	-	0.0350	0.048	-	0.011	0.014	-	0.50	0.3
B1	P	Smooke	-	0.0250	0.035	-	0.008	0.010	-	0.50	0.3
C1	P	Smooke	-	0.0250	0.035	-	0.008	0.010	-	0.50	0.3

Table 2: Oxidiser composition for the MILD mixture.

Cases	$X_{O_2,ox}$	$X_{H_2O,ox}$	$X_{CO_2,ox}$	$X_{N_2,ox}$
A1-2	0.049	0.123	0.062	0.765
AZ1-2, B1, C1	0.035	0.134	0.067	0.764
BZ1	0.020	0.146	0.073	0.761

The numerical domain for all cases except case C1 is a cuboid of size $L_x \times L_y \times L_z = 10 \times 10 \times 10$ mm^3 with inflow and non-reflecting Navier-Stokes Characteristics Boundary Conditions outflow [20] in the x-direction and periodic conditions in the transverse, y and z, directions. This domain is presented in Fig. 1 where the iso-surface of normalised heat release is shown.

Table 3: Turbulence and temperature conditions for the MILD combustion DNS. Λ_0: the integral lengthscale; u': root-mean square of the velocity fluctuations; Re_t and Re_λ: turbulent and Taylor microscale Reynolds numbers respectively.

Cases	Λ_0 [mm]	u' [m/s]	Re_t	Re_λ	T_r [K]
A2	1.63	10.12	67	26	1500
C1	2.52	4.10	55	28.83	1300
Other	1.42	16.67	96	34.73	1500

This figure will be discussed in details in section 4. For case C1, the domain is $30 \times 20 \times 20$ mm^3. To ensure that all chemical and turbulence lengthscales are resolved, a uniform grid of 384^3 for case B1, 756×504^2 for case C1 and 512^3 for the other cases is used to discretized the numerical domain [9, 10]. The MS-58 mechanism presented in [10] is used to describe the methane-air combustion chemistry for the non-premixed MILD combustion cases (AZ1, AZ2 and BZ1) while the Smooke and Giovangigli mechanism [21] is used for the premixed cases (A1, A2, B1 and C1). A summary of the DNS conditions for all cases is presented in Table 1.

The numerical code SENGA2 [22] was used to conduct all runs except case C1 which was run using a fully-compressible code, TTX [23]. Each case was run for about 2.0 flow-through times, $\tau_f = L_x/U_{in}$, where U_{in} is the inflow velocity. $U_{in} = 20$ m/s for the non-premixed cases, 25 m/s for A1, A2 and B1, and 2 m/s for C1. All analysis presented below are based on approximately 50 snapshots for each case taken after statistical convergence is achieved.

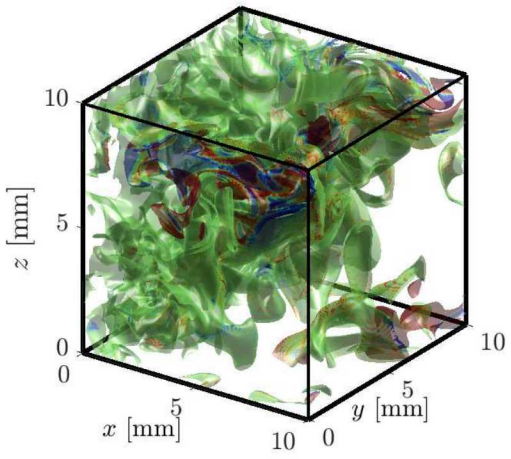

Figure 1: Iso-surfaces of normalised heat release rate $\dot{Q}^+ = 2.0$, at $t = 1.5\tau_f$ for case AZ1. The surface is coloured depending on the value of the CEMA-indicator α defined in section 3 (red: $\alpha > 1$, green: $|\alpha| < 1$, blue: $\alpha < -1$).

3. CEMA Methodology

The analysis of combustion modes is based on CEMA originally proposed by Lu et al. [18]. CEMA is based on the analysis of the eigenvalues, λ_e, of the Jacobian of the local chemical source term, $\boldsymbol{J}_{\boldsymbol{\omega}}$, in the governing equations. This has been extended to account for diffusion effects to distinguish between combustion modes [13, 14]. This is obtained from:

$$\frac{D\boldsymbol{\omega}(\boldsymbol{y})}{Dt} = \boldsymbol{J}_{\boldsymbol{\omega}} \frac{D\boldsymbol{y}}{Dt} = \boldsymbol{J}_{\boldsymbol{\omega}}(\boldsymbol{\omega} + \boldsymbol{s}), \quad \boldsymbol{J}_{\boldsymbol{\omega}} = \frac{\partial \boldsymbol{\omega}}{\partial \boldsymbol{y}} \tag{1}$$

where $\boldsymbol{y}$ represents the species concentrations and temperature, $\boldsymbol{\omega}$ is the chemical source term and $\boldsymbol{s}$ is the non-chemical term representing effects such as diffusion or homogeneous mixing. A Chemical Explosive Mode (CEM) exists if the eigenvalue of the Jacobian, λ_e, has a positive real part. To distinguish between the different combustion modes, Eq. (1) is projected in

the direction of the corresponding left eigenvectors, $\boldsymbol{b_e}$, of $\boldsymbol{J_\omega}$:

$$\boldsymbol{b_e} \cdot \frac{D\boldsymbol{\omega}(\boldsymbol{y})}{Dt} = \boldsymbol{b_e} \cdot \boldsymbol{J_\omega}(\boldsymbol{\omega} + \boldsymbol{s}) = \lambda_e \boldsymbol{b_e} \cdot (\boldsymbol{\omega} + \boldsymbol{s}) \tag{2}$$

Then, the expression for the projected source term is:

$$\frac{D\phi_\omega}{Dt} = \lambda_e \phi_\omega + \lambda_e \phi_s + \frac{D\boldsymbol{b_e}}{Dt} \cdot \boldsymbol{\omega}(\boldsymbol{y}) \tag{3}$$

where $\phi_\omega = \boldsymbol{b_e} \cdot \boldsymbol{\omega}$ and $\phi_s = \boldsymbol{b_e} \cdot \boldsymbol{s}$ are respectively the projected chemical and diffusion terms. The ratio $\alpha = \phi_s/\phi_\omega$ can then be used to indicate the relative importance of diffusion and chemistry and based on the values of α, three regimes can be identified: $\alpha > 1$ for assisted-ignition mode where diffusion dominates chemistry and promotes ignition, $|\alpha| < 1$ for autoignition where chemistry is predominant and $\alpha < -1$ for local extinction mode, where diffusion suppresses ignition. Details regarding this method can be found in [13].

4. Results

4.1. Laminar flames

Figure 2 shows the profiles of the projected chemical and diffusion source terms for a 1D freely propagating laminar methane-air premixed flames with a reactant temperature of 300 K and for a burner-stabilised laminar MILD combustion methane-diluted air (oxidiser of case AZ1 in Table 2) flame with a reactant temperature of 1500K. Both cases are for a lean mixture with equivalence ratio of $\phi = 0.8$ and were computed using CANTERA. The reaction front is indicated as the zero-crossing of λ_e from positive to negative values and the local combustion modes are shown only for explosive mixtures

($\lambda_e > 0$). It is seen that for the case with $T_r = 300$ K, in Fig. 2a, diffusion dominates chemistry for $T < T_i$ where T_i is the temperature where $\phi_s = \phi_\omega$. This indicates that the ignition of the flame is initiated through diffusion processes. However, it is interesting to note that even for this propagating flame, some regions with $|\alpha| < 1$ are observed which suggests that, even for a laminar flame front, the α-indicator will indicate some ignition regions. For the MILD combustion case, it is observed that, in this configuration with low oxygen level, diffusion effects are significantly less important as seen from the lower values of ϕ_s and most of the process is dominated by autoignition.

4.2. 3D MILD combustion DNS

Figure 1 shows typical iso-surfaces of normalised heat release rate, $\dot{Q}^+ = \dot{Q}\delta_{th}/(\rho_r s_L C_p(T_b - T_r)$, for case AZ1, coloured by the α-indicator. The particular aspects of reaction zones in MILD combustion is directly visible with more convoluted reaction zones. This induces frequent reaction zones interaction and more volumetrically distributed reactions as was discussed in [9, 10]. As a consequence, reactions zones in MILD combustion have a larger probability to interact with each other which leads to the apparent volumetrically distributed reaction zones observed [9, 10]. In addition, it is seen that there are large variations of α on those isosurfaces indicating that these reaction zones originate both from ignition (green) and deflagration (red) modes. Other cases show similar features for the reaction zones.

This is further assessed in Fig. 3 which shows the α-distribution in the mid x-y plane for explosive regions ($\lambda_e > 0$) for cases AZ1, AZ2 and B1. It is seen that most cases exhibit large autoignition regions ($\alpha \approx 0$) with patches of deflagrative structures ($\alpha \geq 1$). However, the premixed case B1, in Fig.

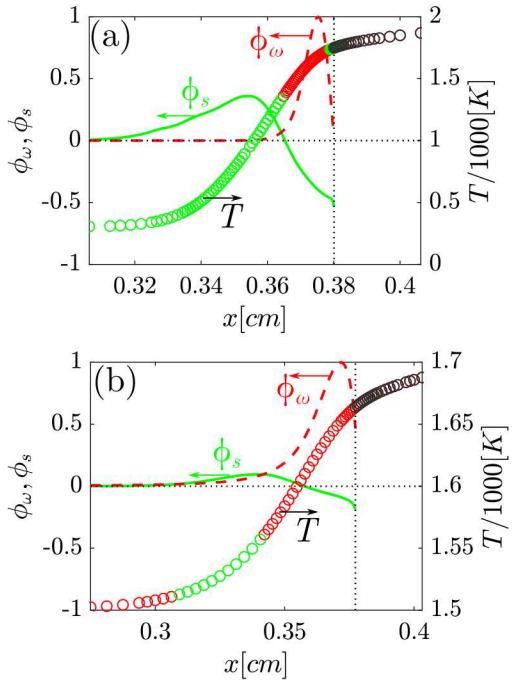

Figure 2: Profiles of chemical and diffusion projection terms with temperature for 1-D freely propagating laminar premixed flame for a (a) methane-air flame at $\phi = 0.8$ and $T_r = 300$ K, and (b) for the MILD combustion mixture at $\phi = 0.8$ and $T_r = 1500$ K. Temperature profiles are coloured by α (red: $|\alpha| < 1$, green: $|\alpha| > 1$). Grey circle: regions where $\lambda_e < 0$ and α is not computed there.

3c, shows that the deflagrative mode is more likely in the upstream region of the domain when compared with the non-premixed cases. The fraction of extinguishing regions ($\alpha \leq -1$) is small compared to the other combustion modes. It should be noted that, while these regions are extinguishing at that particular time, these mixtures may still further mix and react again at a later time, further downstream [11].

The specific dominant mode of each case is further analysed in Fig. 4 where the PDF of α is shown. It is constructed using spatial samples with

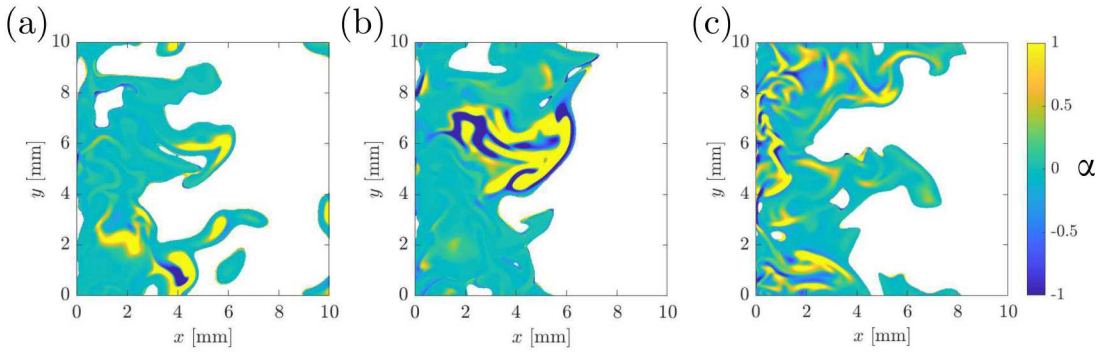

Figure 3: Distribution of α in regions with $\lambda_e > 0$ in the mid x-y plane at $t = 1.5\tau_f$ for cases (a) AZ1, (b) AZ2 and (c) B1.

$\lambda_e > 0$ to only account for chemically active regions. Furthermore, regions with $\alpha > 1$ and $\alpha < -1$ are set to $+1$ or -1 respectively to allow for a clear comparison of the various possible combustion modes (ignition, flame propagation and extinction). It is seen that, overall, cases AZ1 and AZ2 show that $\alpha \geq 1$, and thus flame propagation, is the most likely mode but that both ignition and deflagration are nearly balanced. Case BZ1 and all the other premixed cases show that $\alpha = 0$, and thus ignition, is the most important combustion mode.

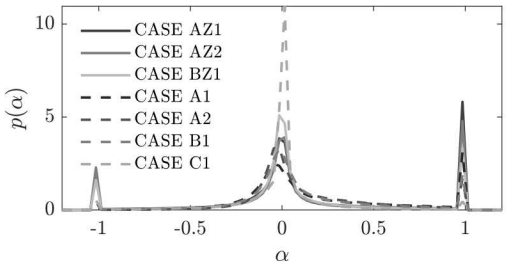

Figure 4: PDF of α in regions with $\lambda_e > 0$ for all cases at $t = 1.5\tau_f$.

The previous analysis showed the global behaviour of the various com-

bustion cases. However, there are strong spatial variations of α as previously seen in Fig. 3. This is analysed in Fig. 5 which shows the PDF of α for some specific axial locations for representative cases. Figure 5a shows the behaviour of case B1 which is representative of all premixed cases. In that figure, it is observed that, as one moves downstream, the peak probability of α shifts from 0 to a slightly positive value while the probability of deflagration decreases. This indicates that premixed MILD combustion is ignition dominated for the various O_2 levels, turbulence intensities and reactant temperatures considered. This makes premixed MILD combustion similar to HCCI systems and suggests that premixed MILD combustion can be reliably modelled using a PSR or PaSR approaches. For case AZ1, in Fig. 5b, it is seen that as one traverses downstream, ignition (the peak of $p(\alpha) = 0$) becomes less important while flame propagation becomes dominant. This indicates that ignition kernels evolve into propagating flames for this case. A somewhat similar behaviour is also observed for case BZ1 (not shown here). Conversely, Fig. 5c shows that, upstream, there is a balance of ignition and propagating flames and that as one traverses downstream, ignition remains dominant. This indicates the existence of sequential autoignition, similar to the physics of PCCI systems with mixture fraction stratification [24] or in HCCI systems with temperature stratification [25]. This stems from the stronger mixture fraction stratification in case AZ2 as it has a smaller ℓ_Z as indicated in Table 1. This hinders the development of flame fronts. Furthermore, because of this stronger mixture stratification, the various pockets of mixtures undergo ignition independently depending on their mixture fraction and local conditions [11]. This analysis shows that, in MILD combustion, the

combustion mode is mainly influenced by the mixture fraction stratification. Indeed, all premixed cases exhibit a similar dominant ignition mode, irrespective of the turbulence or O_2 levels, supporting previous studies [9]. On the other hand, when introducing a mixture fraction stratification, either a mixed ignition/deflagration mode or a sequential autoignition mode were observed depending on the typical lengthscale of the mixture fraction field. The various findings here support the observation made in previous work where the relative importance of the combustion mode was studied using a balance between the diffusion/convection and reaction terms in the species transport equation [9, 11].

To further analyse the specific effect of the mixture fraction on the combustion mode, the PDF of mixture fraction conditioned on the combustion mode identified using α is shown in Fig. 6. This shows that ignition ($|\alpha| < 1$) is mostly present in lean mixtures which is consistent with conventional autoignition where lean mixtures are more likely to ignite [26]. On the other hand, deflagrative structures ($\alpha > 1$) are mostly present in rich mixtures. This further emphasizes that combustion models for non-premixed MILD combustion should be able to handle both combustion modes.

Finally, the fractional contribution of the various combustion modes to the total heat release rate in the entire domain is presented in Table 4. It is observed that, despite the large probability of finding a deflagrative mode observed in Fig. 4, those regions contributes to a very small portion of the total heat release rate in the computational domain where over 85% of the total heat release rate is due to autoignition. This indicates that while there may be a distribution of deflagrative modes, MILD combustion is

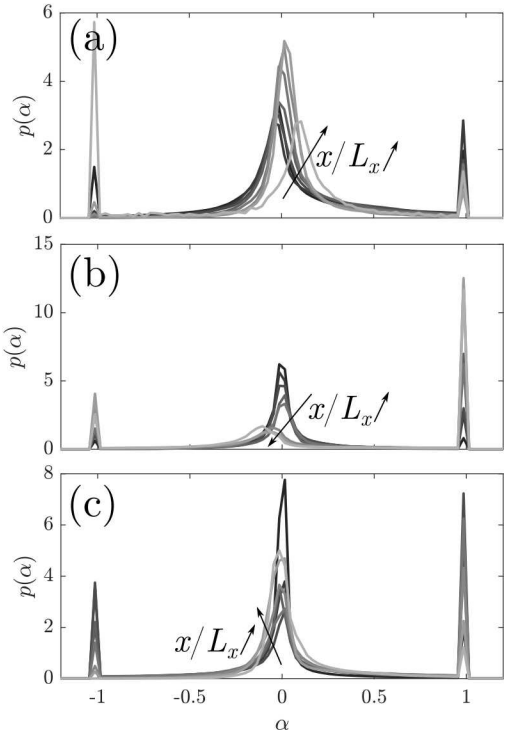

Figure 5: Evolution of $p(\alpha)$ at various axial locations: $x/L_x = 0.03125,\ 0.15625, ...,\ 0.90625$ (from upstream to downstream: black to light gray) for cases (a) B1, (b) AZ1 and (c) AZ2 at $t = 1.5\tau_f$.

predominantly controlled by ignition processes. This trend is slightly stronger for the premixed cases with $T_r = 1500$ K, and strongest for the premixed case with $T_r = 1300$ K. This supports the present finding that for the premixed MILD cases considered in this study, ignition is dominant irrespective of the local thermochemical and turbulence conditions.

5. Conclusion

The CEMA methodology has been applied to DNS data of MILD combustion to study the specific balance between ignition and flame propagation in

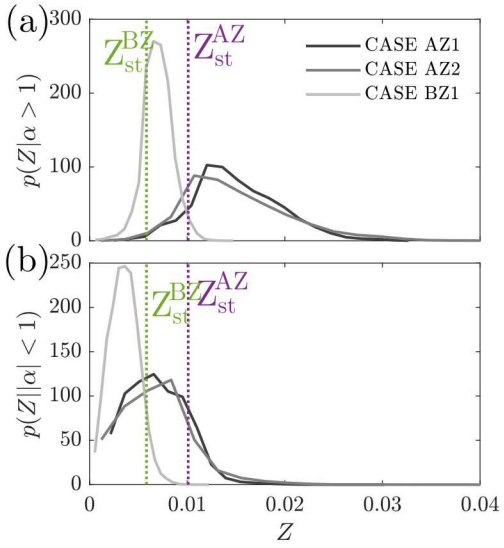

Figure 6: PDF of Z conditioned on (a) $\alpha > 1$, (b) $|\alpha| < 1$ and (c) $\alpha < -1$. Vertical lines indicate the stoichiometric mixture fraction for the cases AZ1-2 and BZ.

Table 4: Fractional contribution of the various combustion modes to the total heat release rate in the domain for all MILD combustion cases.

CASE	$\mathcal{Q}_{fl}$	$\mathcal{Q}_{ign}$	$\mathcal{Q}_{ext}$
AZ1	0.0753	0.8877	0.0370
AZ2	0.0551	0.9111	0.0338
BZ1	0.0503	0.9258	0.0239
A1	0.0436	0.9430	0.0134
A2	0.0274	0.9593	0.0052
B1	0.0311	0.9673	0.0096
C1	0.0067	0.9869	0.0064

MILD combustion. This analysis relies on the identification of the eigenvalues of the Jacobian of the chemical source term and the delineation between ignition and deflagration. First, from laminar analysis, it is observed that a

MILD combustion mixture with lower oxygen content reacts as an autoigniting mixture and diffusion-assisted reactions are much less important than in a conventional methane-air mixture. Subsequently, applying this analysis to 3D DNS of MILD combustion showed that autoignition is the most important mode of combustion for all cases considered, but the deflagration mode remains non-negligible. This supports previous findings in [9, 11] which highlighted similar features using an indicator based on a balance of the convective-diffusive and reactive effects. Furthermore, it was observed that for premixed MILD combustion case, the combustion mode is neither strongly dependent on oxygen nor turbulence levels indicating, that all premixed MILD combustions are mostly ignition dominated. However, in the case of MILD combustion with mixture fraction stratification, a strong influence of the mixture fraction and axial location on the α distribution was observed. Indeed, for cases AZ1 and BZ1 which have $\ell_Z > \ell_c$, it is observed that as one moves downstream the probability of having autoigniting regions decreases while deflagration becomes more prominent. This indicates that the initial ignition kernels develop into propagating flames. On the other hand, case AZ2 which has a smaller ℓ_Z, showed that ignition remains the most dominant mode even in the downstream part of the domain. This is because of the sequential autoignition of the various pockets of reacting mixture undergoing autoignition at different times depending on their autoignition delay times. Finally, it was observed that lean mixtures are strongly correlated with ignition while stoichiometric or rich mixtures are more likely to undergo deflagration under MILD conditions.

These observations also suggest that PSR or PaSR based model would be

applicable for premixed MILD combustion but that for non-premixed conditions, both ignition and deflagration need to be accounted for to model MILD combustion adequately. Furthermore, analysing species that are aligned with the chemical explosive mode could help identify potential markers to distinguish between ignition and deflagration. Finally, analogously to the study of [25] for HCCI with temperature stratification, relating the gradient of ignition delay time due to mixture fraction stratification to the sequential ignition would be interesting. This will be the topic for future work.

Acknowledgement

N.A.K.D. acknowledges the support of the TUM-IAS, funded by the German Excellence Initiative and the EU 7th Framework Programme under grant agreement no. 291763. This work used the ARCHER UK National Supercomputing Service (http://www.archer.ac.uk) under RAP project e419 and UKCTRF e305. Y.M. acknowledges the support of JSPS Grant-in-Aid for Young Scientists (B) Grant Number 19K14903.

References

[1] A. Cavaliere, M. de Joannon, Mild Combustion, Prog. Energy Combust. Sci. 30 (2004) 329–366.

[2] A. A. V. Perpignan, A. Gangoli Rao, D. J. E. M. Roekaerts, Flameless combustion and its potential towards gas turbines, Prog. Energy Combust. Sci. 69 (2018) 28–62.

[3] M. Katsuki, T. Hasegawa, The science and technology of combustion in highly preheated air, 27th Symp. Combust. 27 (1998) 3135–3146.

[4] C. Duwig, B. Li, Z. S. Li, M. Aldén, High resolution imaging of flameless and distributed turbulent combustion, Combust. Flame 159 (2012) 306–316.

[5] P. R. Medwell, P. A. M. Kalt, B. B. Dally, Simultaneous imaging of OH, formaldehyde, and temperature of turbulent nonpremixed jet flames in a heated and diluted coflow, Combust. Flame 148 (2007) 48–61.

[6] P. R. Medwell, P. A. M. Kalt, B. B. Dally, Imaging of diluted turbulent ethylene flames stabilized on a Jet in Hot Coflow (JHC) burner, Combust. Flame 152 (2008) 100–113.

[7] E. Oldenhof, M. J. Tummers, E. H. van Veen, D. J. E. M. Roekaerts, Ignition kernel formation and lift-off behaviour of jet-in-hot-coflow flames, Combust. Flame 157 (2010) 1167–1178.

[8] J. A. M. Sidey, E. Mastorakos, Visualization of MILD combustion from jets in cross-flow, Proc. Combust. Inst. 35 (2015) 3537–3545.

[9] Y. Minamoto, N. Swaminathan, R. S. Cant, T. Leung, Morphological and statistical features of reaction zones in MILD and premixed combustion, Combust. Flame 161 (2014) 2801–2814.

[10] N. A. K. Doan, N. Swaminathan, Y. Minamoto, DNS of MILD combustion with mixture fraction variations, Combust. Flame 189 (2018) 173–189.

[11] N. A. K. Doan, N. Swaminathan, Autoignition and flame propagation in non-premixed MILD combustion, Combust. Flame 201 (2019) 234–243.

[12] M. U. Göktolga, J. A. van Oijen, L. P. H. de Goey, 3D DNS of MILD combustion: A detailed analysis of heat loss effects, preferential diffusion, and flame formation mechanisms, Fuel 159 (2015) 784–795.

[13] C. Xu, J. W. Park, C. S. Yoo, J. H. Chen, T. Lu, Identification of premixed flame propagation modes using chemical explosive mode analysis, Proc. Combust. Inst. 37 (2019) 2407–2415.

[14] K. Aditya, A. Gruber, C. Xu, T. Lu, A. Krisman, M. R. Bothien, J. H. Chen, Direct numerical simulation of flame stabilization assisted by autoignition in a reheat gas turbine combustor, Proc. Combust. Inst. 37 (2019) 2635–2642.

[15] C. Xu, A. Y. Poludnenko, X. Zhao, H. Wang, T. Lu, Structure of strongly turbulent premixed n-dodecaneair flames: Direct numerical simulations and chemical explosive mode analysis, Combust. Flame 209 (2019) 27–40.

[16] S. Hartl, D. Geyer, A. Dreizler, G. Magnotti, R. S. Barlow, C. Hasse, Regime identification from Raman/Rayleigh line measurements in partially premixed flames, Combust. Flame 189 (2018) 126–141.

[17] C. S. Yoo, E. S. Richardson, R. Sankaran, J. H. Chen, A DNS study on the stabilization mechanism of a turbulent lifted ethylene jet flame in highly-heated coflow, Proc. Combust. Inst. 33 (2011) 1619–1627.

[18] T. F. Lu, C. S. Yoo, J. H. Chen, C. K. Law, Three-dimensional direct numerical simulation of a turbulent lifted hydrogen jet flame in heated

coflow: a chemical explosive mode analysis, J. Fluid Mech. 652 (2010) 45–64.

[19] D. J. Diamantis, D. C. Kyritsis, D. A. Goussis, The reactions supporting or opposing the development of explosive modes: Auto-ignition of a homogeneous methane/air mixture, Proc. Combust. Inst. 35 (2015) 267–274.

[20] T. Poinsot, Boundary conditions for direct simulations of compressible viscous flows, J. Comput. Phys. 101 (1992) 104–129.

[21] M. D. Smooke, V. Giovangigli, Formulation of the premixed and non-premixed test problems, in: M. D. Smooke (Ed.), Reduc. Kinet. Mech. Asymptot. Approx. Methane-Air Flames, volume 384 of *Lecture Notes in Physics*, Springer Berlin Heidelberg, Berlin/Heidelberg, 1991, pp. 1–28.

[22] R. S. Cant, SENGA2 User Guide (CUED-THERMO-2012/04, 2nd ed.), Technical Report, University of Cambridge, 2013.

[23] M. Tanahashi, M. Fujimura, T. Miyauchi, Coherent fine-scale eddies in turbulent premixed flames, Proc. Combust. Inst. 28 (2000) 529–535.

[24] M. B. Luong, G. H. Yu, S. H. Chung, C. S. Yoo, Ignition of a lean PRF/air mixture under RCCI/SCCI conditions: Chemical aspects, Proc. Combust. Inst. 36 (2017) 3587–3596.

[25] J. H. Chen, E. R. Hawkes, R. Sankaran, S. D. Mason, H. G. Im, Direct numerical simulation of ignition front propagation in a constant volume with temperature inhomogeneities I . Fundamental analysis and diagnostics, Combust. Flame 145 (2006) 128–144.

[26] E. Mastorakos, Ignition of turbulent non-premixed flames, Prog. Energy Combust. Sci. 35 (2009) 57–97.

Declaration of interests

☒ The authors declare that they have no known competing financial interests or personal relationships that could have appeared to influence the work reported in this paper.

☐The authors declare the following financial interests/personal relationships which may be considered as potential competing interests: